

# FINAL-STRUCTURE PREDICTION OF CONTINUOUSLY CAST BILLETS

## NAPOVED KONČNE MIKROSTRUKTURE KONTINUIRNO ULITIH GREDCI

Josef Štětina, Lubomír Klimeš, Tomáš Mauder, František Kavička

Brno University of Technology, Technická 2, 616 69 Brno, Czech Republic  
stetina@fme.vutbr.cz

Prejem rokopisa – received: 2011-10-20; sprejem za objavo – accepted for publication: 2012-01-09

In steel production, controlling and monitoring quality, grade and structure of final steel products are very important issues. It has been shown that the temperature distribution, the magnitude of temperature gradients, as well as the cooling strategy during the continuous steel casting have a significant impact on material properties, the structure and any defect formation of cast products. The paper describes an accurate computational tool intended for investigating the transient phenomena in continuously cast billets, for developing the caster control techniques and also for determining the optimum cooling strategy in order to meet all quality requirements. The numerical model of the temperature field is based on the finite-difference implementation of the 3D energy-balance equation using the enthalpy approach. This allows us to analyse the temperature field along the entire cast billet. Since the steel billets are produced constantly 24 hours per day, the transient temperature field is being computed in a non-stop trial run. It enables us to monitor and investigate the formation of the temperature field in real time within the mould, as well as the secondary and tertiary cooling zones, where the observed information can be immediately utilized for the caster-control optimization with respect to the whole machine or just an individual part. The application of the presented model is demonstrated with two examples including the steelworks in Trinec, Czech Republic, and in Podbrezová, Slovakia. To consider different operational conditions, the influences of the secondary-cooling setting on the surface and the inner defects formation, and on the final structure of the 150 × 150 mm billet are also discussed.

Keywords: concast billet, numerical model, solidification

Pri proizvodnji jekla je pomembno izvajanje kontrole kvalitete, vrste in mikrostrukture končnih proizvodov. Prikazano je, da ima razporeditev temperature, razpon temperaturnega gradienta, kot tudi strategija ohlajanja med kontinuirnim ulivanjem pomemben vpliv na lastnosti materiala, mikrostrukturo in možnost nastanka napak v litem proizvodu. V članku je predstavljeno natančno računalniško orodje za preiskave prehodnih pojavov v kontinuirno uliti gredici. Orodje je namenjeno razvoju kontrolne tehnike in tudi za določanje optimalne strategije ohlajanja za doseganje zahtevane kakovosti. Numerični model temperaturnega polja temelji na uporabi končnih diferenc 3D-enačbe energijskega ravnotežja z uporabo entalpije. Omogoča analizo temperaturnega polja vzdolž celotne lite gredice. Ker je proizvodnja gredic stalna, 24 ur na dan, je bilo prehodno temperaturno polje izračunano za neprekinjeno preskusno obratovanje. Omogočena je kontrola in preiskava nastanka temperaturnega polja v realnem času v kokili, v sekundarni in terciarni hladilni coni. Ugotovljena informacija se lahko neposredno uporabi za optimiranje celotne livne naprave ali pa samo posameznega dela. Uporaba predlaganega modela je prikazana za dva primera iz železarne Trinec na Češkem in železarne Podbrezová na Slovaškem. Prikazan je tudi vpliv nastavitve sekundarnega ohlajanja na nastanek površinskih in notranjih napak na gredici 150 mm × 150 mm pri različnih obratovalnih razmerah.

Ključne besede: kontinuirno ulite gredice, numerični model, strjevanje

### 1 NUMERICAL MODEL OF THE TEMPERATURE FIELD OF A CONCAST BILLET

The presented in-house model of the transient temperature field of the blank from a billet caster (**Figure 1**) is unique. In addition to being entirely 3D, it can operate in real time. It is possible to adapt its universal code and use it for any billet caster. The numerical model covers the temperature field of the entire length of a blank (i.e., from the meniscus inside the mould all the way down to the cutting torch) with up to one million nodes.

The solidification and cooling of a blank and the simultaneous heating of the mould is a case of the 3D transient heat and mass transfer in a system comprising a blank-mould ambient and, after leaving the mould, only a blank ambient<sup>1</sup>. If mass transfer is neglected and if only conduction is considered as being decisive, then the heating up of the mould is described by the Fourier

Equation (1). The solidification and the cooling of a blank is described by the Fourier-Kirchhoff Equation (2),

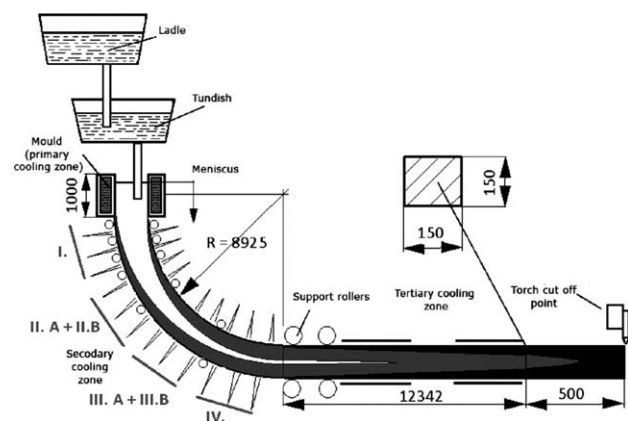


Figure 1: A billet caster

Slika 1: Shematski prikaz kontinuirnega ulivanja gredic

which contains the components describing the heat flow from the melt flowing with a velocity  $v$ , and the component including the internal source of latent heats of phase or structural changes  $\dot{Q}_{source}$ .

$$\rho \cdot c \frac{\partial T}{\partial \tau} = \frac{\partial}{\partial x} \left( k \frac{\partial T}{\partial x} \right) + \frac{\partial}{\partial y} \left( k \frac{\partial T}{\partial y} \right) + \frac{\partial}{\partial z} \left( k \frac{\partial T}{\partial z} \right) \quad (1)$$

$$\rho \cdot c \frac{\partial T}{\partial \tau} = \frac{\partial}{\partial x} \left( k \frac{\partial T}{\partial x} \right) + \frac{\partial}{\partial y} \left( k \frac{\partial T}{\partial y} \right) + \frac{\partial}{\partial z} \left( k \frac{\partial T}{\partial z} \right) + \rho \cdot c \left( u \frac{\partial T}{\partial x} + v \frac{\partial T}{\partial y} + w \frac{\partial T}{\partial z} \right) + \dot{Q}_{source} \quad (2)$$

**Figure 2** shows the temperature balance of an elementary volume representing the general node of the mesh  $(i,j,k)$  inside the mould. The heat conductivities  $VX$ ,  $VY$  and  $VZ$  along the main axes are:

$$VX_{i,j,k} = k_i \frac{A_x}{\Delta x} \quad VX_{i-1,j,k} = k_{i-1} \frac{A_x}{\Delta x} \quad (3a)$$

$$VY_{i,j,k} = k_j \frac{A_y}{\Delta y} \quad VY_{i,j-1,k} = k_{j-1} \frac{A_y}{\Delta y} \quad (3b)$$

$$VZ_{i,j,k} = k_k \frac{A_z}{\Delta z} \quad VZ_{i,j,k-1} = k_{k-1} \frac{A_z}{\Delta z} \quad (3c)$$

The heat flows  $QX$ ,  $QY$  and  $QZ$  through the elementary volume along the main axes are:

$$QX = VX_{i,j,k} (T_{i+1,j,k}^{(\tau)} - T_{i,j,k}^{(\tau)}) \quad (4a)$$

$$QY_i = VY_{i,j,k} (T_{i,j+1,k}^{(\tau)} - T_{i,j,k}^{(\tau)}) \quad (4b)$$

$$QX1 = VX_{i-1,j,k} (T_{i-1,j,k}^{(\tau)} - T_{i,j,k}^{(\tau)}) \quad (4c)$$

$$QY1 = VY_{i,j-1,k} (T_{i,j-1,k}^{(\tau)} - T_{i,j,k}^{(\tau)}) \quad (4d)$$

$$QZ_{i,j} = VZ_{i,j,k} (T_{i,j,k+1}^{(\tau)} - T_{i,j,k}^{(\tau)}) \quad (4e)$$

$$QZ1_{i,j} = VZ_{i,j,k-1} (T_{i,j,k-1}^{(\tau)} - T_{i,j,k}^{(\tau)}) \quad (4f)$$

The temperature balance of the general node is:

$$\frac{(QZ1_{i,j} + QZ_{i,j} + QY1_{i,j} + QY_{i,j} + QX1 + QX)}{\Delta x \cdot \Delta y \cdot \Delta z \cdot \rho \cdot c} = \frac{\partial T}{\partial \tau} (T_{i,j,k}^{(\tau+\Delta\tau)} - T_{i,j,k}^{(\tau)}) \quad (5)$$

where the right-hand side expresses the accumulation (or loss) of heat in the node  $i,j,k$  during the time step  $\Delta\tau$ . The unknown temperature of the general node of the

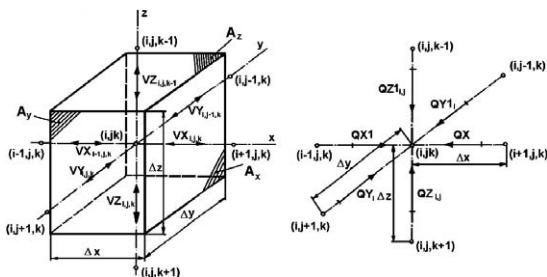


**Figure 2:** Heat balance of the general node of the mesh  
**Slika 2:** Diagram toplotnega ravnovesja v splošni točki mreže

mesh inside the mould in the following instant  $(\tau + \Delta\tau)$  is therefore given by the explicit formula:

$$T_{i,j,k}^{(\tau+\Delta\tau)} = T_{i,j,k}^{(\tau)} + \frac{(QZ1_{i,j} + QZ_{i,j} + QY1_{i,j} + QY_{i,j} + QX1 + QX)}{\Delta x \cdot \Delta y \cdot \Delta z \cdot \rho \cdot c} \cdot \Delta\tau \quad (6)$$

The temperature field of the blank passing through a radial caster of a large radius can be simplified by the Fourier-Kirchhoff equation where only the  $v_z$  component of the velocity is considered. Equation (2) is therefore reduced to:

$$\rho \cdot c \frac{\partial T}{\partial \tau} = \frac{\partial}{\partial x} \left( k \frac{\partial T}{\partial x} \right) + \frac{\partial}{\partial y} \left( k \frac{\partial T}{\partial y} \right) + \frac{\partial}{\partial z} \left( k \frac{\partial T}{\partial z} \right) + \rho \cdot c \cdot w \frac{\partial T}{\partial z} + \dot{Q}_{source} \quad (7)$$

Equation (7) must cover the temperature field of the blank in all three stages: above the liquidus temperature (i.e., the melt), in the interval between the liquidus and solidus temperatures (i.e., the so-called mushy zone) and beneath the solidus temperature (i.e., the solid phase). It is therefore convenient to introduce the thermodynamic function of specific volume enthalpy  $H_v = cpT$ , which is dependent on temperature, and also includes the phase and structural heats (**Figure 3**).

Heat conductivity  $k$ , specific heat capacity  $c$  and density  $\rho$  are thermophysical properties that are also functions of temperature. Equation (7) therefore takes on the form:

$$\frac{\partial H_v}{\partial \tau} = \frac{\partial}{\partial x} \left( k \frac{\partial T}{\partial x} \right) + \frac{\partial}{\partial y} \left( k \frac{\partial T}{\partial y} \right) + \frac{\partial}{\partial z} \left( k \frac{\partial T}{\partial z} \right) + w \frac{\partial H_v}{\partial z} \quad (8)$$

The heat balance of the elementary node is:

$$\frac{(QZ1_{i,j} + QZ_{i,j} + QY1_{i,j} + QY_{i,j} + QX1 + QX)}{\Delta x \cdot \Delta y \cdot \Delta z} = \frac{\partial T}{\partial \tau} (T_{vi,j,k}^{(\tau+\Delta\tau)} - T_{vi,j,k}^{(\tau)}) \quad (9)$$

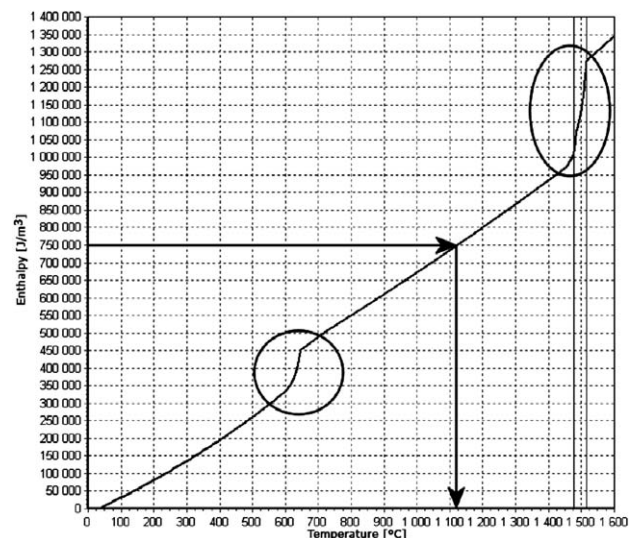


**Figure 3:** The enthalpy function for steel showing the phase and structural changes  
**Slika 3:** Entalpijska funkcija za jeklo s fazno in strukturno premeno

where the heat flow  $QZ_{i,j}$  must now also include the enthalpy of the incoming volume of melt:

$$(QZ)_{i,j} = QZ_{i,j}(T_{i,j,k+1}^{(\tau)} - T_{i,j,k}^{(\tau)}) - A_z \cdot w \cdot H_{vi,j,k}^{(\tau)} \quad (10)$$

The unknown enthalpy of the general node of the blank in the following instant  $(\tau + \Delta\tau)$  is given by the explicit formula, similar to Equation (6):

$$H_{vi,j,k}^{(\tau + \Delta\tau)} = H_{vi,j,k}^{(\tau)} + (QZ)_{i,j} + QZ_{i,j} + QY_{i,j} + QX_{i,j} + QX_{i,j} \cdot \frac{\Delta\tau}{\Delta x \cdot \Delta y \cdot \Delta z} \quad (11)$$

**Figure 3** indicates how the temperature model for the calculated enthalpy in Equation (11) determines the unknown temperature.

The next task is to choose a suitable coordinate system and a mesh. This paper deals with the symmetrical half of one cross-section of a blank from the meniscus inside the mould down to the cutting torch. The origin of the coordinate system is positioned on the small radius in the centre of the width (**Figure 4**). This enables all coordinates to be positive, which facilitates the software programming. In the region of the radius, the Cartesian coordinates are transformed into the cylindrical ones (i.e.,  $y$  is the radius and  $z$  is the angle). The mesh is generated automatically and the model supports all densities of the mesh introduced in **Figure 4**. All the results presented in this paper are based on a mesh of 573,594 nodes (11 in the  $x$ -direction, 21 in the  $y$ -direction and 1861 in the  $z$ -direction) and a  $7.5 \text{ mm} \times 7.5 \text{ mm} \times 15 \text{ mm}$  elementary volume.

All thermodynamic properties of the cast steel, dependent on its chemical composition and the cooling rate, enter the calculation as functions of temperature<sup>2</sup>. This is therefore a significantly non-linear task because, even with the boundary conditions, their dependence on the surface temperature of the blank is considered here.

Regarding the fact that the task can be considered symmetrical along the axis (**Figure 4**), it is sufficient to deal with only one half of the cross-section. The boundary conditions are therefore as follows:

$$1. T = T_{\text{cast}} \quad \text{the level of the steel} \quad (12a)$$

$$2. -k \frac{\partial T}{\partial n} = 0 \quad \text{the plane of symmetry} \quad (12b)$$

$$3. -k \frac{\partial T}{\partial n} = htc \cdot (T_{\text{surface}} - T_{\text{amb}}) \quad \text{inside the mould} \quad (12c)$$

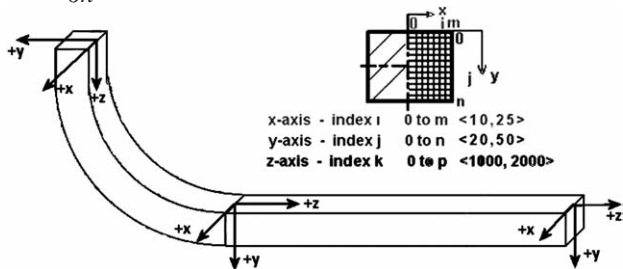


**Figure 4:** The mesh and the definition of the coordinate system  
**Slika 4:** Mreža in opredelitev koordinatnega sistema

$$4. -k \frac{\partial T}{\partial n} = htc \cdot (T_{\text{surface}} - T_{\text{amb}}) + \sigma \epsilon (T_{\text{surface}}^4 - T_{\text{amb}}^4) \quad \text{within the secondary and tertiary zones} \quad (12d)$$

$$5. -k \frac{\partial T}{\partial z} = \dot{q} \quad \text{beneath the rollers} \quad (12e)$$

The boundary conditions are divided into the area of the mould, the area of the secondary cooling and the area of the tertiary cooling.

The initial condition for the investigation is the setting of the temperature in individual points of the mesh. A suitable temperature is the highest possible temperature, i.e., the pouring temperature. The explicit difference method is used for solving this problem. The principle of this method is that the stability of the calculation is dependent on the magnitude of the time step. The model has incorporated a method for adapting the time step, i.e., the time step entered by the operator is merely a recommendation and the software modifies it throughout the calculation.

## 2 HEAT TRANSFER COEFFICIENT ALONG THE ENTIRE CASTER

The cooling by the water nozzles has the main influence and it is therefore necessary to devote much attention to establishing the relevant heat-transfer coefficient of the forced convection. Commercially sold models of the temperature field describe the heat-transfer coefficient beneath the nozzles as a function of the incident quantity of water per unit area. They are based on various empirical relationships. This procedure is undesirable. The model discussed in this paper obtains its heat-transfer coefficients from the measurements of spraying characteristics of all nozzles used by the caster on the so-called hot plate in an experimental laboratory<sup>3,4</sup> and for a sufficient range of operational pressures of water, as well as for a sufficient range of casting speeds of the blank (i.e., casting speed). This approach represents a unique combination of an experimental measurement in a laboratory and a numerical model for calculating the non-linear boundary conditions beneath the cooling nozzle.

**Figure 5** presents the measured values of the heat-transfer coefficients processed by the temperature-model software. For the nozzle configuration, there is a graph of the heat-transfer coefficient beneath the nozzle. These graphs are plotted for a surface temperature of  $1000 \text{ }^\circ\text{C}$ .

The resultant heat-transfer coefficient is determined by adding up the partial coefficients. This basically entails the total heat-transfer coefficient because even radiation, with the introduction of the "reduced heat-transfer coefficient from radiation", was converted to convection. On the areas of the blank, where the natural convection and radiation occur, the total coefficient is given by the sum of the reduced coefficient from radiation and the coefficient of the actual natural convection.

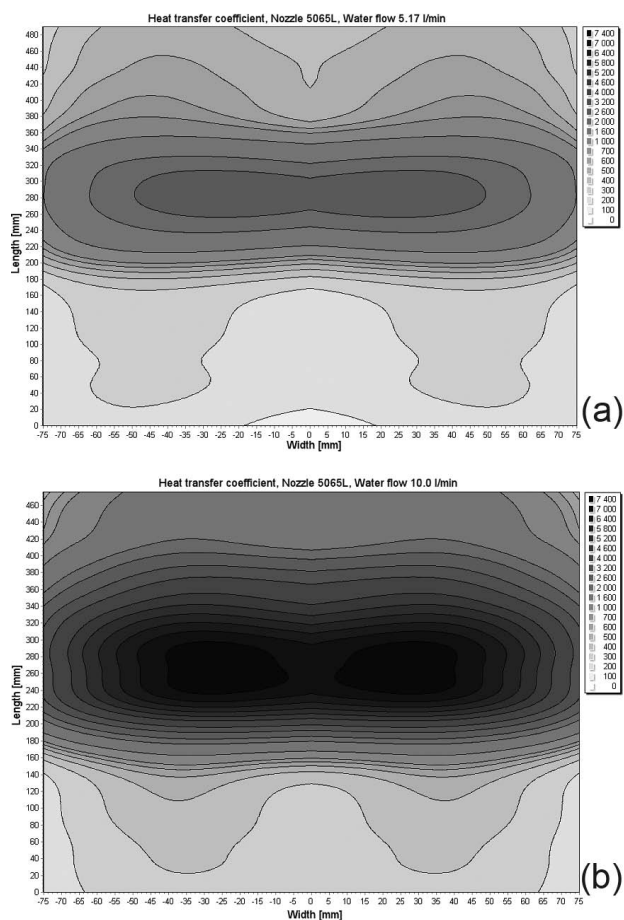


**Figure 5:** The heat-transfer coefficient for the 50651 nozzle: a) flow through a nozzle at 5.17 L/min, b) flow through a nozzle at 10.00 L/min

**Slika 5:** Koeficient prehoda toplote za šobo 50651: a) pretok skozi eno šobo pri 5,17 L/min, b) pretok skozi eno šobo pri 10,00 L/min

In the area beneath the nozzle, the resultant heat-transfer coefficient is obtained as the sum of the forced-convection coefficient gained from the laboratory-temperature measurement and the reduced heat-transfer coefficient from radiation<sup>2</sup>.

On a specific caster, the nozzles of the secondary cooling are divided into several independent regulation zones, enabling the formation of the temperature field of the blank. **Figure 6** shows the 6 individual regulation zones and **Figure 7** shows the courses of the resultant heat-transfer coefficients along the small radius of the billet caster. On a specific caster, the nozzles of the secondary cooling are divided into several independent regulation zones (I, IIA, IIB, IIIA, IIIB and IV), enabling the formation of the temperature field of the blank.<sup>5</sup>

### 3 EFFECT OF THE SECONDARY COOLING

The setting of the secondary cooling and its optimization is a very complicated problem<sup>6</sup>. In a real operation specific intensity of cooling is characterized by the consumption of the cooling water per 1 kg of cast

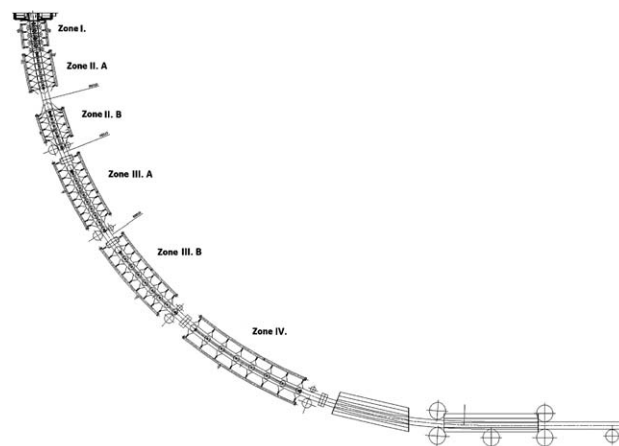


**Figure 6:** Positions of the nozzles along the billet caster in 6 individual zones

**Slika 6:** Pozicije hladilnih šob vzdolž naprave za ulivanje gredic v 6 območjih

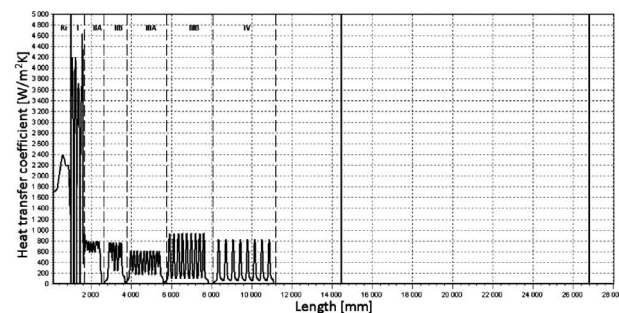


**Figure 7:** The resultant heat-transfer coefficient along the small radius of the billet caster

**Slika 7:** Dobljeni koeficienti prehoda toplote vzdolž notranjega radija naprave za ulivanje gredic

steel. On the basis of the curves indicating various consumptions of cooling water per unit of the mass of cast steel varying from 9 L/kg to 18 L/kg, the temperature of the blank was calculated and presented in **Figure 8**. These cooling curves are established for the given caster referring to six cooling zones I, IIA, IIB, IIIA, IIIB and IV.

### 4 ON-LINE MODEL OF THE TEMPERATURE FIELD

A temperature model can be considered to be successfully implemented if it is integrated into the existing information and control systems of a caster. The users (i.e., technologists) can record the real-time data from the on-line model into their off-line model of the temperature field, carry out any necessary changes in the input parameters (e.g., alter the secondary cooling or the casting speed). After a simulation on the off-line model, it is possible to determine how the temperature field will change after the implementation of the changes. Another application of the off-line version is in the occurrence of defects on/in the actual slab or sheet steel. The user can

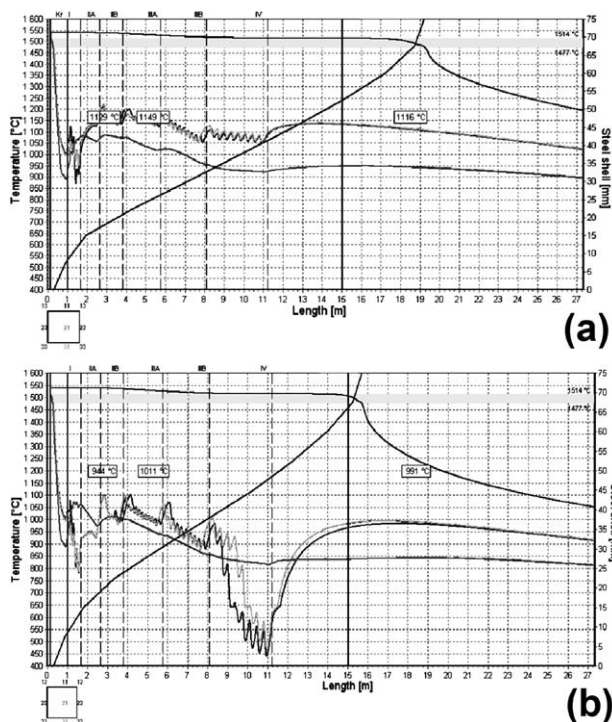


**Figure 8:** A comparison of the temperature fields with different intensities of secondary cooling: a) cooling curve 9 L/kg, b) cooling curve 18 L/kg

**Slika 8:** Primerjava temperaturnih polj pri različni intenzivnosti sekundarnega hlajenja: a) krivulja ohlajanja pri 9 L/kg, b) krivulja ohlajanja pri 18 L/kg

read the temperature field from the archive server using the dynamic model and – using the off-line model – analyse any likely causes of defects and prepare the necessary measures for the defects never to occur again. The off-line model will (in future) enable the reading of quantities and their dependences from the application server and, using statistical methods and the relationships among these quantities and defects, will look for

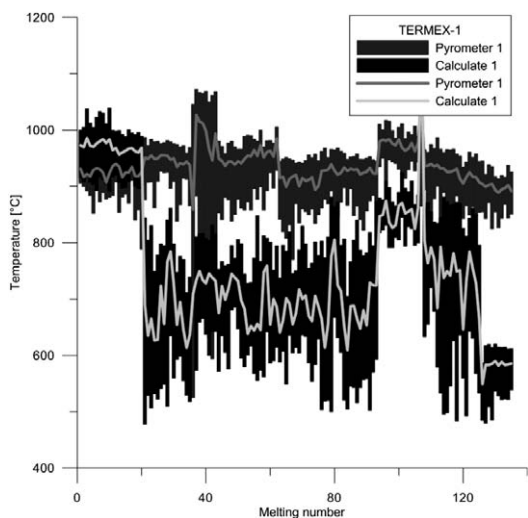


**Figure 9:** The measured and calculated temperatures of a billet  
**Slika 9:** Izmerjene in izračunane temperature gredice

the cause in the original temperature field of the con-casting from a specific melt. However, this will be the task of the mathematical-stochastic prediction model.

**Figure 9** compares the average values of the measured surface temperatures in the same points. Comparing the absolute values, it is possible to see that there are long intervals where the deviation is significant and, on the other hand, there are intervals where the values are identical.

## 5 CONCLUSIONS

This paper presents a 3D numerical model of the temperature field (for con-casting of steel) in the form of an in-house software that has been implemented in the operation of TRINECKÉ ŽELEZÁRNY, Czech Republic and in Podbrezová, Slovakia. The model deals with the main thermodynamic transfer phenomena during the solidification of con-casting.

Our analysis proved the usefulness of the model for real applications, as well as the reliability and robustness of the used numerical methods and other software. The model has been applied in the calculation and setting of the constants of the caster control system, including the simulation of the caster operation under non-standard situations (e.g., partial failures of the secondary cooling during an unexpected slowing down of the casting), in the planned maintenance of the machine or its structural improvements, in the utilization of the information that helps the operator to make spontaneous changes to the control of the machine, in the utilization of monitoring and controlling the quality, in the direct control of the casting speed and in the flow of water in individual zones of the secondary cooling of the prediction system<sup>7</sup>.

## Acknowledgments

This analysis was conducted by using a program devised within the framework of the project GA CR No. 106/08/0606, 106/09/0940 and P107/11/1566, NETME centre – New Technologies for Mechanical Engineering CZ.1.05/2.1.00/01.0002, Specific research BUT BD13102003 and the co-author, the holder of Brno PhD Talent Financial Aid sponsored by Brno City Municipality.

## Nomenclature

- $A/m^2$  – area
- $c/(J/kg\ K)$  – specific heat capacity
- $htc/(W/m^2\ K)$  – heat transfer coefficient
- $H_v/(J/m^3)$  – volume enthalpy
- $k/(W/mK)$  – heat conductivity
- $T/K$  – temperature
- $T_{amb}/K$  – ambient temperature
- $T_{cast}/K$  – melt temperature
- $T_{surface}/K$  – temperature in unbending part

$\dot{q}/(\text{W}/\text{m}^2)$  – specific heat flow

$QX/W, QY/W, QZ/W$  – heat flows

$\dot{Q}_{\text{source}}/(\text{W}/\text{m}^3)$  – internal heat source

$x/\text{m}, y/\text{m}, z/\text{m}$  – axes in given direction

$u/(\text{m}/\text{s}), v/(\text{m}/\text{s}), w/(\text{m}/\text{s})$  – casting speed in given direction

$VX/(\text{W}/\text{K}), VY/(\text{W}/\text{K}), VZ/(\text{W}/\text{K})$  – heat conductivity

$\rho/(\text{kg}/\text{m}^3)$  – density

$\sigma/(\text{W}/\text{m}^2 \text{K}^4)$  – Stefan-Boltzmann constant

$\varepsilon$  – emissivity

$\tau/\text{s}$  – time

## 6 REFERENCES

- <sup>1</sup> J. K. Brimacombe, The Challenge of Quality in Continuous Casting Process, *Metallurgical and Materials Trans. B*, 30B (1999), 553–566
- <sup>2</sup> J. Miettinen, S. Louhenkilpi, J. Laine, Solidification analysis package IDS. Proceeding of General COST 512 Workshop on Modelling in Materials Science and Processing, M. Rappaz and M. Kedro eds., ECSC-EC-EAEC, Brussels, Luxembourg, 1996
- <sup>3</sup> M. Prihoda, J. Molinek, R. Pyszko, M. Velicka, M. Vaculík, J. Burda, Heat Transfer during Cooling of Hot Surfaces by Water Nozzles, *Metalurgija = Metallurgy*, 48 (2009) 4, 235–238
- <sup>4</sup> J. Horsky, M. Raudensky, Measurement of Heat transfer Characteristics of Secondary Cooling in Continuous Casting. In *Metal 2005*. Ostrava: TANGER, 2006, 1–8
- <sup>5</sup> A. Richard, Kai Liu Harding, Ch. Beckermann, A transient simulation and dynamic spray cooling control model for continuous steel casting, *Metallurgical and materials transactions*, 34B (2003), 297–302
- <sup>6</sup> F. Kavička, J. Stetina, B. Sekanina, K. Stransky, J. Dobrovska, J. Heger, The optimization of a concasting technology by two numerical models, *Journal of Materials Processing Technology*, 185 (2007) 1–3, 152
- <sup>7</sup> B. G. Thomas, R. J. O'Malley, D. T. Stone, Measurement of temperature, solidification, and microstructure in a continuous cast thin slab. Paper presented at Modeling of Casting, Welding and Advanced Solidification Processes VIII, San Diego, CA, TMS 1998